

***In Vivo* Visualization of Tumor Antigen-containing Microparticles Generated in  
Fluorescent-protein-elicited Immunity**

Fei Yang<sup>1,2</sup>, Shun Liu<sup>1,2</sup>, Xiuli Liu<sup>1,2</sup>, Lei Liu<sup>1,2</sup>, Meijie Luo<sup>1,2</sup>, Shuhong Qi<sup>1,2</sup>, Guoqiang Xu<sup>1,2</sup>, Sha Qiao<sup>1,2</sup>,  
Xiaohua Lv<sup>1,2</sup>, Xiangning Li<sup>1,2</sup>, Ling Fu<sup>1,2</sup>, Qingming Luo<sup>1,2,\*</sup>, Zhihong Zhang<sup>1,2,\*</sup>

<sup>1</sup> Britton Chance Center for Biomedical Photonics, Wuhan National Laboratory for Optoelectronics–Huazhong  
University of Science and Technology, Wuhan 430074, China

<sup>2</sup> MoE Key Laboratory for Biomedical Photonics, Department of Biomedical Engineering, Huazhong University of  
Science and Technology, Wuhan 430074, China

## Supporting Information

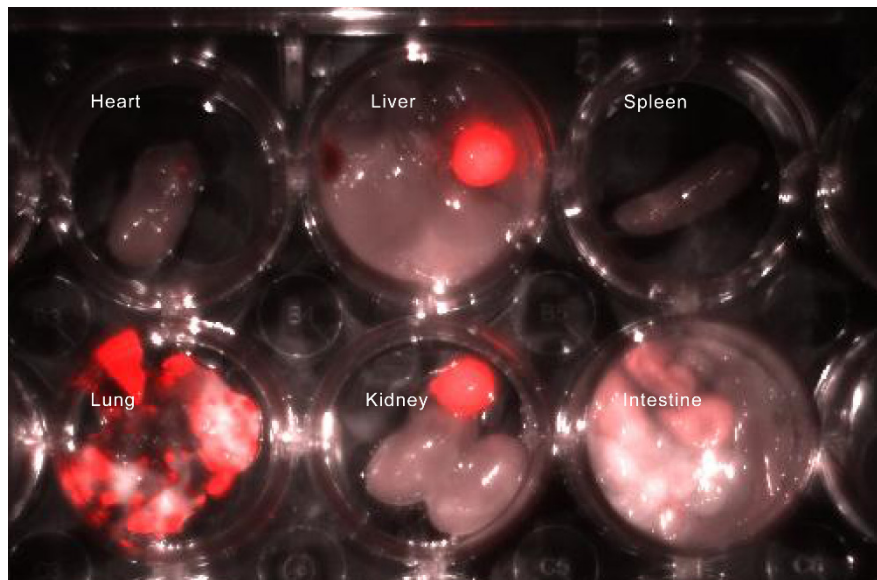


**Figure S1.** tfRFP-B16 metastases in different organs. Visceral metastases generated through the tail vein injection of  $1 \times 10^6$  tfRFP-B16 cells. Data are the representative of at least three mice.

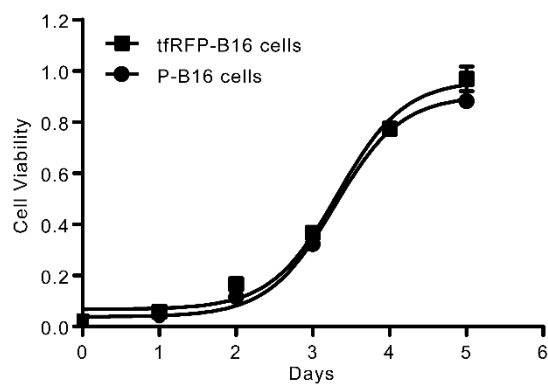


**Figure S2.** tfRFP-B16 and P-B16 cells were demonstrated to have no significant difference in proliferation in vitro. Cell viability of tfRFP-B16 and P-B16 cells at the indicated time points was measured by MTS assay. Data are the representative of three independent experiments.

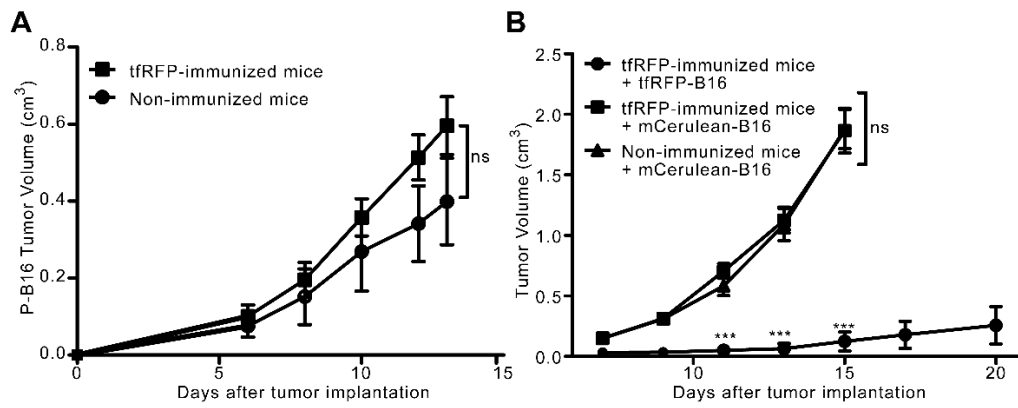


**Figure S3.** tfRFP immunization specifically inhibited the tumorigenesis of tfRFP-B16 cells but not P-B16 or mCerulean-B16 cells in vivo. (A) The tumor growth curves of P-B16 cells in tfRFP-immunized mice and non-immunized mice. (B) The tumor growth curves of mCerulean-B16 cells in the immunized and non-immunized mice and of tfRFP-B16 cells in the immunized mice. For both experiments,  $n = 5$ . The data are the means  $\pm$  SEM. “ns” for  $P > 0.05$ ; \*\*\* for  $P < 0.0001$ .

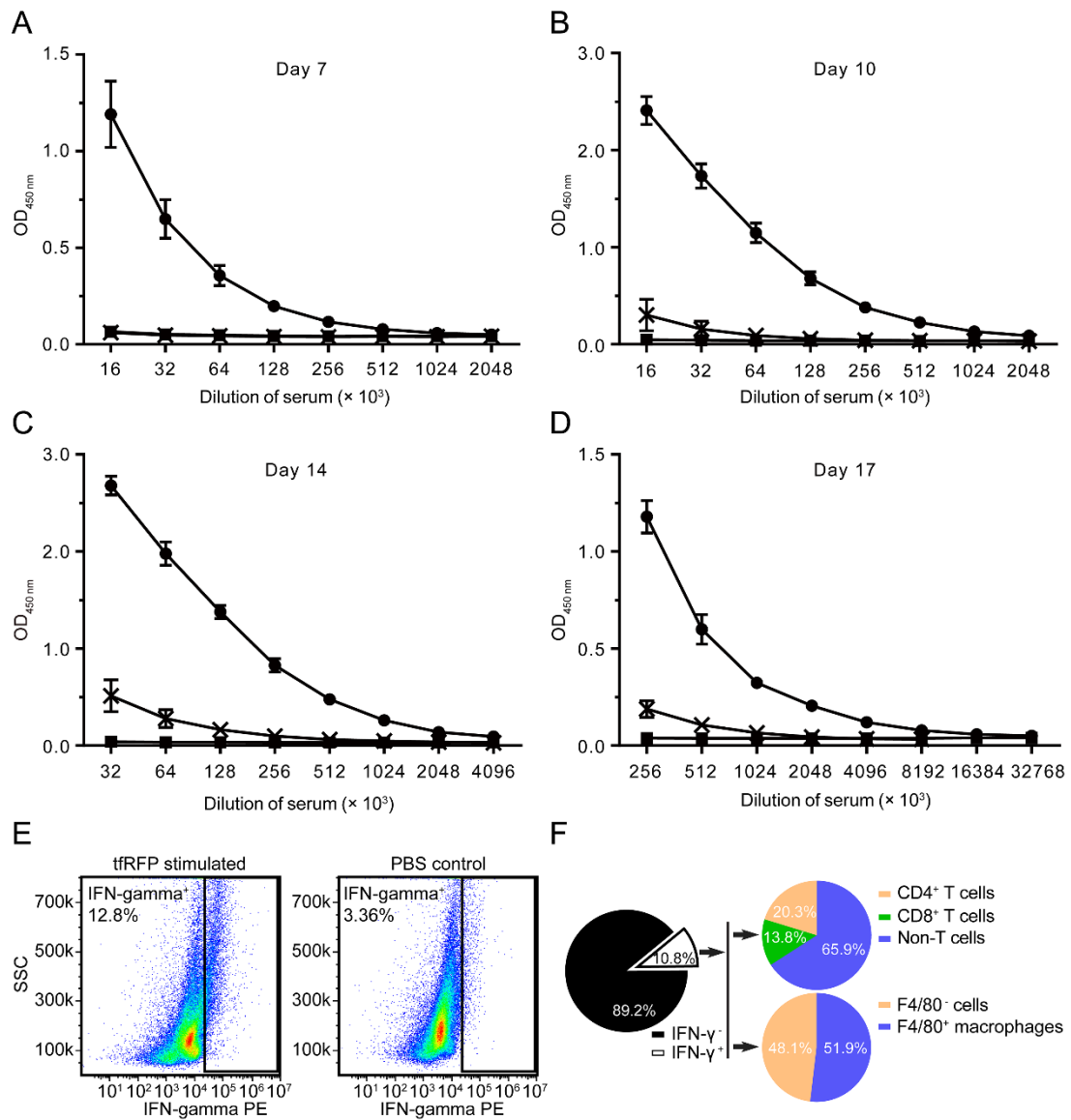


**Figure S4.** Anti-tfRFP antibody titers in the serum and IFN-gamma secretion of splenocytes from tfRFP-immunized mice. (A-D) Serum samples were collected 7 days, 10 days, 14 days, and 17 days after the first immunization from tfRFP-immunized (solid circle), OVA-immunized (cross), and PBS control (solid square) mice and were diluted as indicated and then added to tfRFP-coated plates. The relative quantities of anti-tfRFP or anti-OVA antibody were measured by indirect ELISA. The data are presented as the means  $\pm$  SEM. For the anti-tfRFP antibody, n = 4; for the anti-OVA antibody, n = 3; for the PBS control, n = 3. (E) IFN- $\gamma$  PE<sup>+</sup> splenocyte gating and percentages. The images are the representative of data derived from three mice. (F) The composition analysis of IFN- $\gamma$ <sup>+</sup> splenocytes stimulated with tfRFP. The data were pooled from three mice.

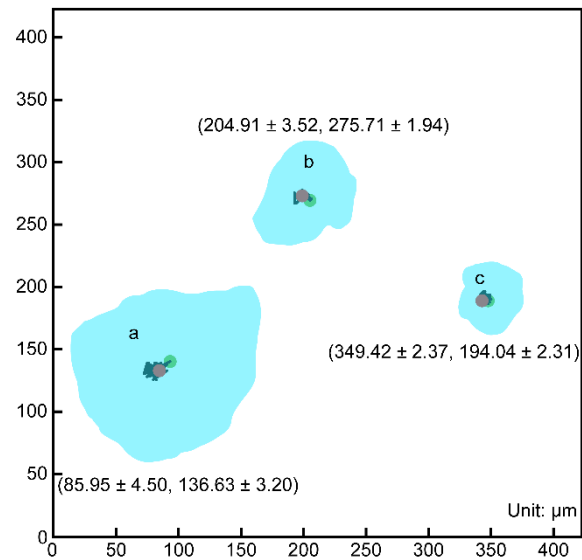


**Figure S5.** The recruitment of neutrophils to form cell clusters around a central point. The formation of cell clusters was presented as the tracks of centroids of each cluster. The starting points of the tracks are indicated with green filled circles, and the ending points are in red. The cyan areas are the regions that each cell cluster covered during the whole imaging session. The ranges of either coordinate of the centroids are presented as the means  $\pm$  SEM near each cluster.

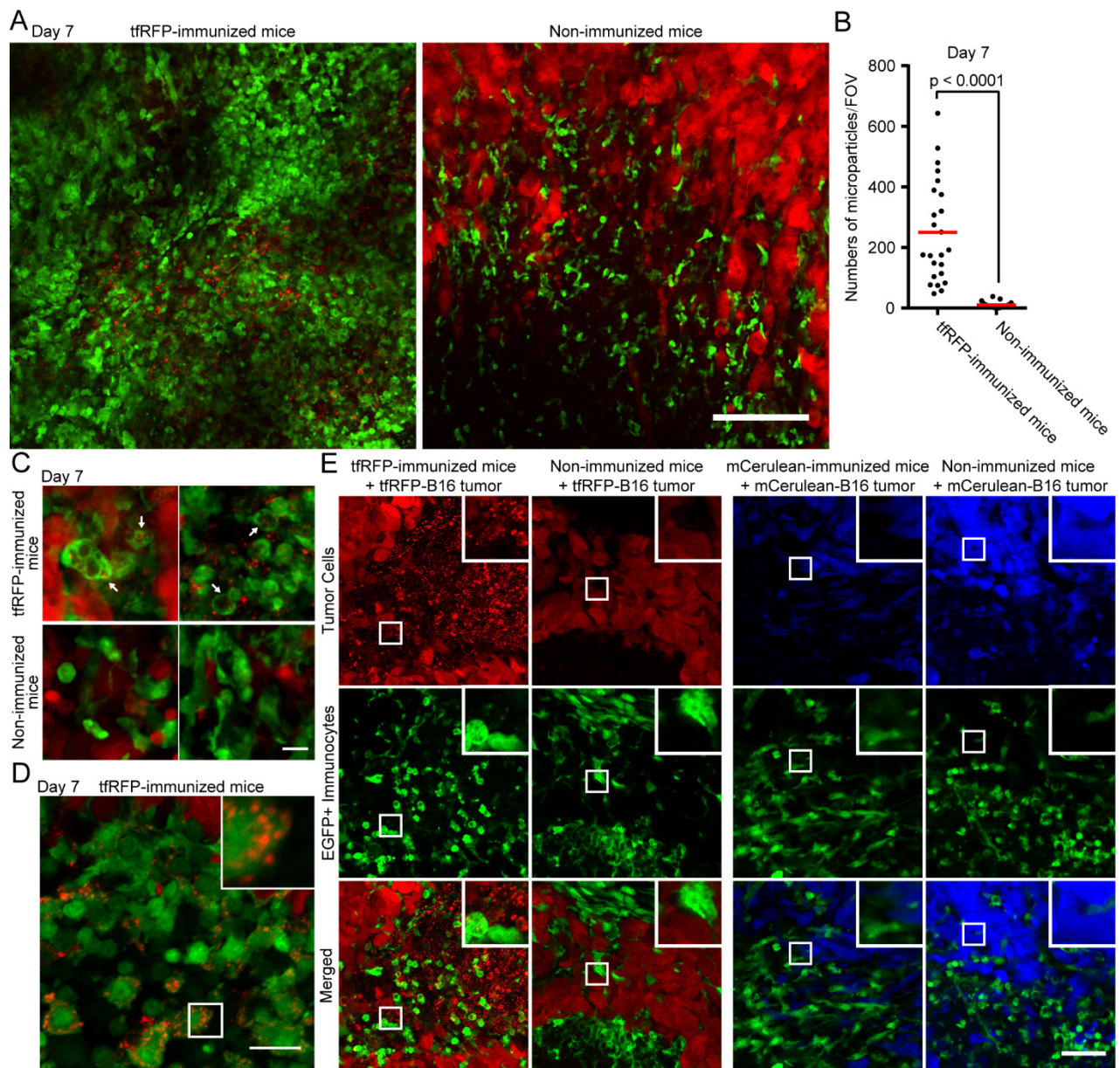


**Figure S6.** Comparison of the microparticles generated in the tFRFP-immunized mice and the non-immunized mice on Day 7. (A) Fluorescent imaging of the tumor cryosections demonstrated that a large number of microparticles were generated in the tFRFP-immunized mice. The scale bar represents 500  $\mu\text{m}$ . (B) Statistical analysis of the number of microparticles per FOV. The size of each FOV is 104.86  $\mu\text{m} \times 104.86 \mu\text{m}$ , zoomed in 4 $\times$  from A. Microparticles of sizes no more than 2  $\mu\text{m}$  were manually enumerated with the aid of ImageJ. Each point stands for the number of microparticles in an FOV. Data are the representative of 4 tFRFP-immunized mice and 3 non-immunized mice. (C) tFRFP<sup>+</sup> microparticles engulfed by EGFP<sup>+</sup> immunocytes in tFRFP-immunized mice but not in non-immunized mice on Day 7 in vivo. The scale bar represents 10  $\mu\text{m}$  in length and 1  $\mu\text{m}$  in height. (D) Fluorescent imaging of tumor cryosections further confirmed the engulfment of tFRFP<sup>+</sup> microparticles by immunocytes in tFRFP-immunized mice on Day 7. The scale bar represents 20  $\mu\text{m}$  in length and 1  $\mu\text{m}$  in height. (E)

The phenomenon of generating microparticles is specific to tfRFP-immunization but not mCerulean-immunization. Day 7 tumors from the indicated mice were separated and sectioned for fluorescent imaging. The images were the representative from 3 mice in each group. The scale bar represents 50  $\mu\text{m}$ .



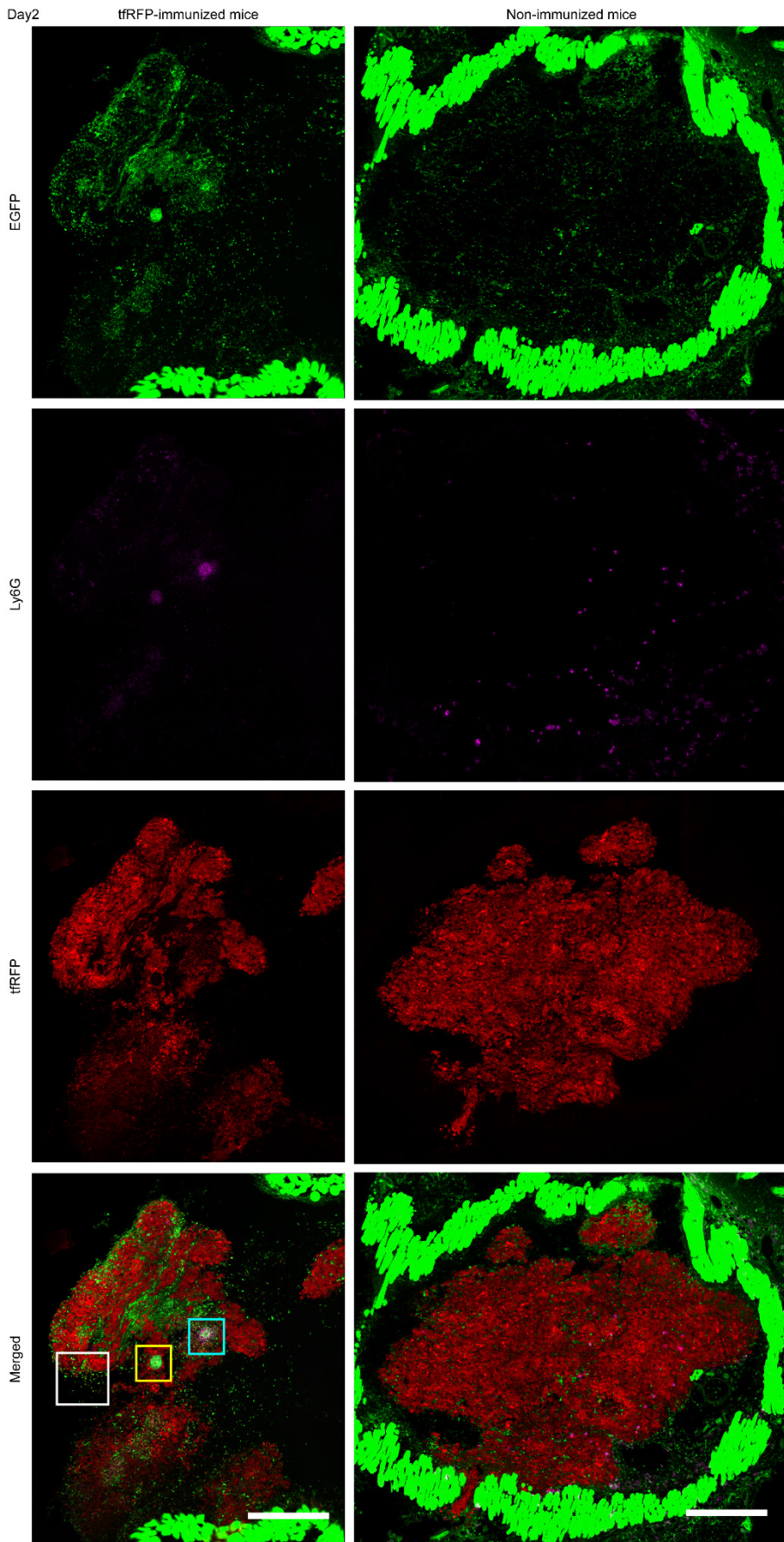


**Figure S7.** Immunofluorescence distribution of Ly6G<sup>+</sup> cells in Day 2 tumor cryosections. Images of whole tumor cryosections were collected with a 20× NA0.8 objective on a Zeiss LSM 710 confocal microscope system. The scale bar represents 500 μm. The yellow and blue boxes are the ROIs shown in Fig. 4B, while the white box shows the FOV of Fig. 4D. The data are representative of 4 mice in each group.



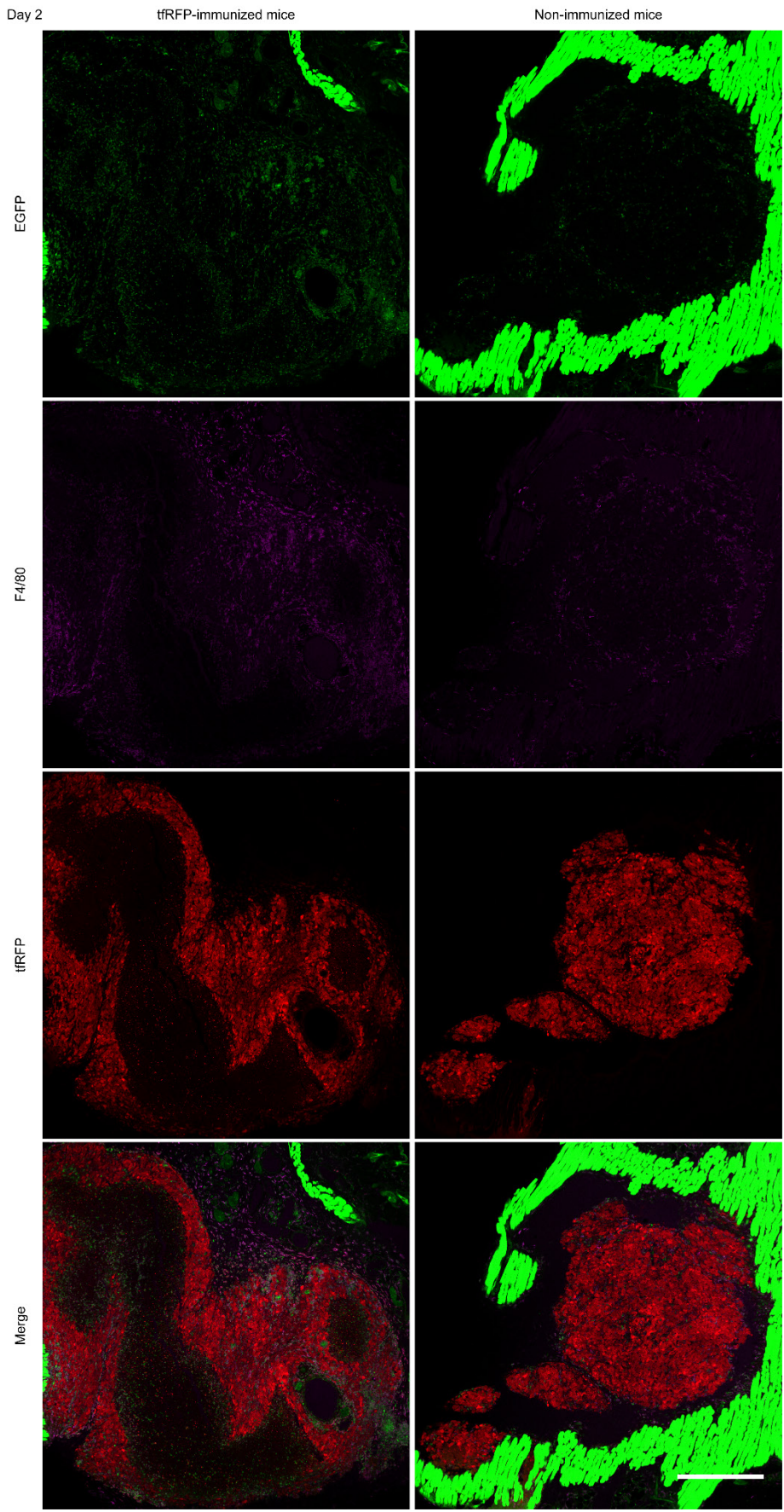


**Figure S8.** Immunofluorescence distribution of F4/80<sup>+</sup> cells in Day 2 tumor cryosections. Images of whole tumor cryosections were collected with a 20× NA0.8 objective on a Zeiss LSM 710 confocal microscope system. The scale bar represents 500 μm. Data are representative of 2 mice in each group.

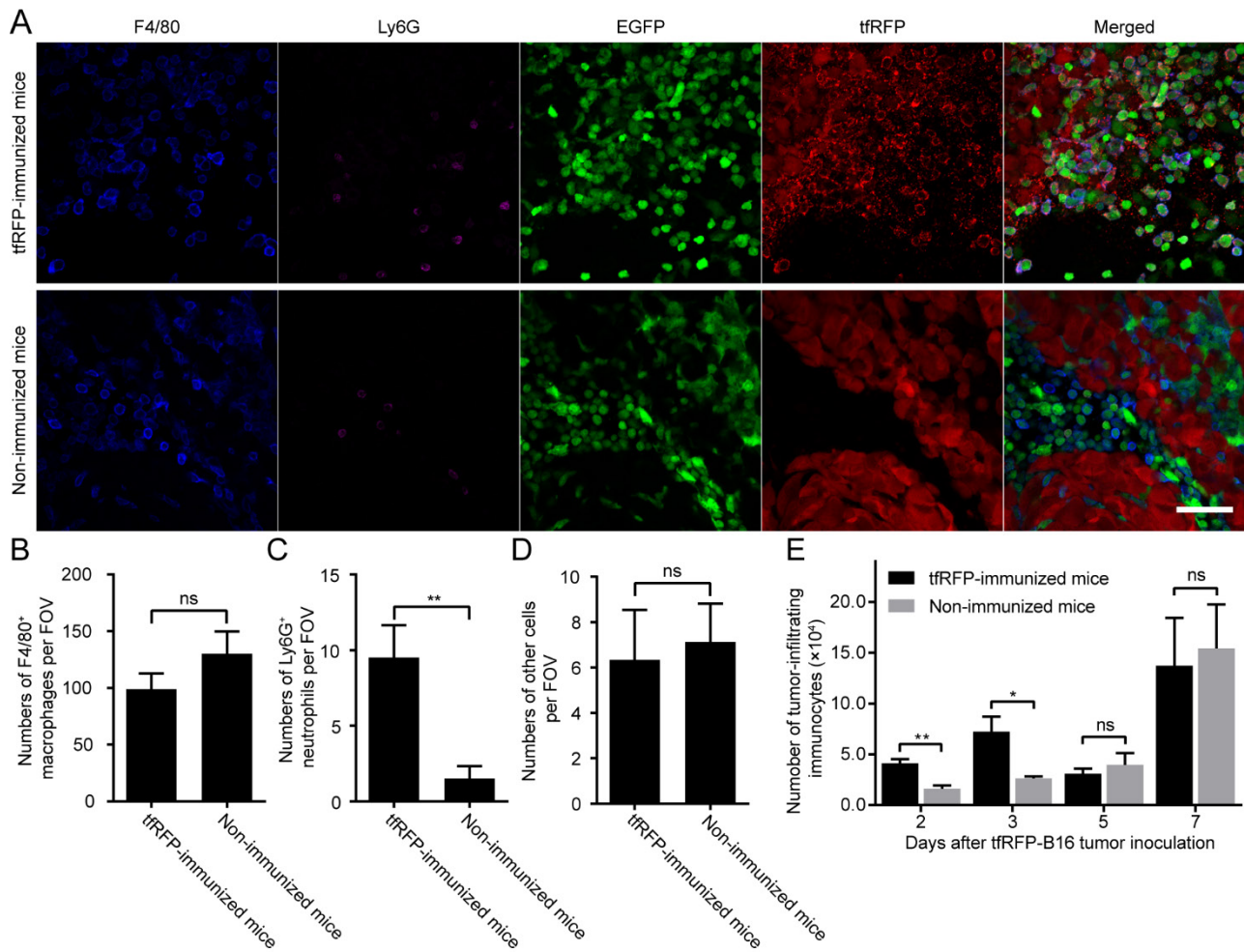


**Figure S9.** Analysis of the make-up of tumor-infiltrating immunocytes in Day-2 tumors. EGFP transgenic mice were immunized and implanted with  $1.0 \times 10^6$  tRF-RFP-B16 cells as previously described. (A) Representative images of the immunofluorescence analysis of tumor sections. The size of the field of view (FOV) is  $212.25 \mu\text{m} \times 212.25 \mu\text{m}$ . The scale bar represents  $50 \mu\text{m}$ . (B-D) Histograms of the numbers of the indicated cell populations in each FOV of 6-8 cryosections from 3 mice in each group that were pooled for statistical analysis. FOVs with cell clusters were excluded from the statistical analysis because it is nearly impossible to enumerate the cells inside. (E) Flow cytometric analysis of the numbers of TIIs at the indicated time points. The data were pooled from 3 mice in each group at each time point. For all the statistical data, the values are presented as the means  $\pm$  SEM.  $P$  values less than 0.05 were considered to be statistically significant ( $*P < 0.05$ ,  $**P < 0.01$ ).



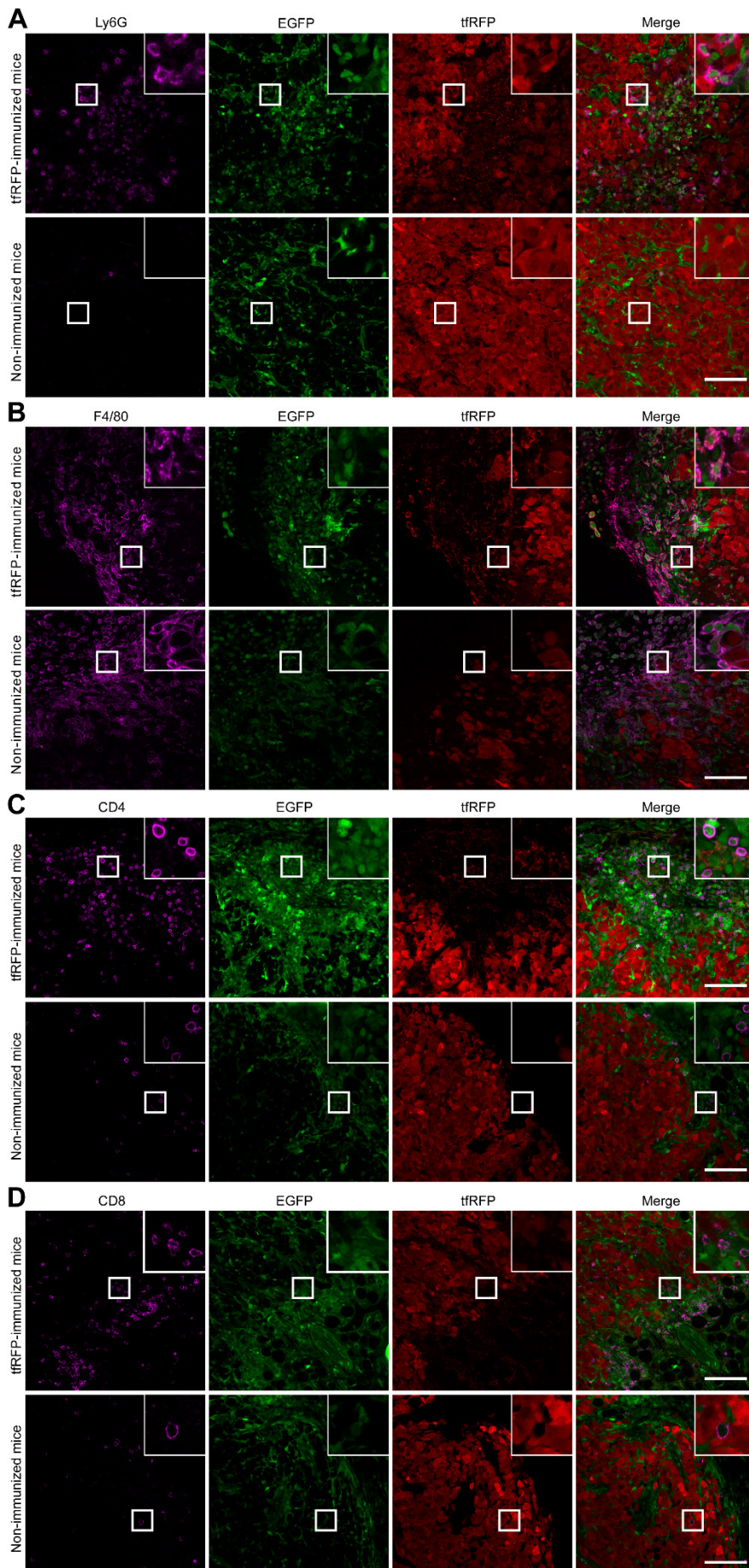


**Figure S10.** Immunofluorescence of distribution of Ly6G<sup>+</sup> neutrophils, F4/80<sup>+</sup> macrophages, CD4<sup>+</sup> T cells or CD8<sup>+</sup> T cells in Day 7 tumor cryosections. The images are corresponding single channel images of each merged image in Fig. 5. All of the scale bars represent 100  $\mu$ m.

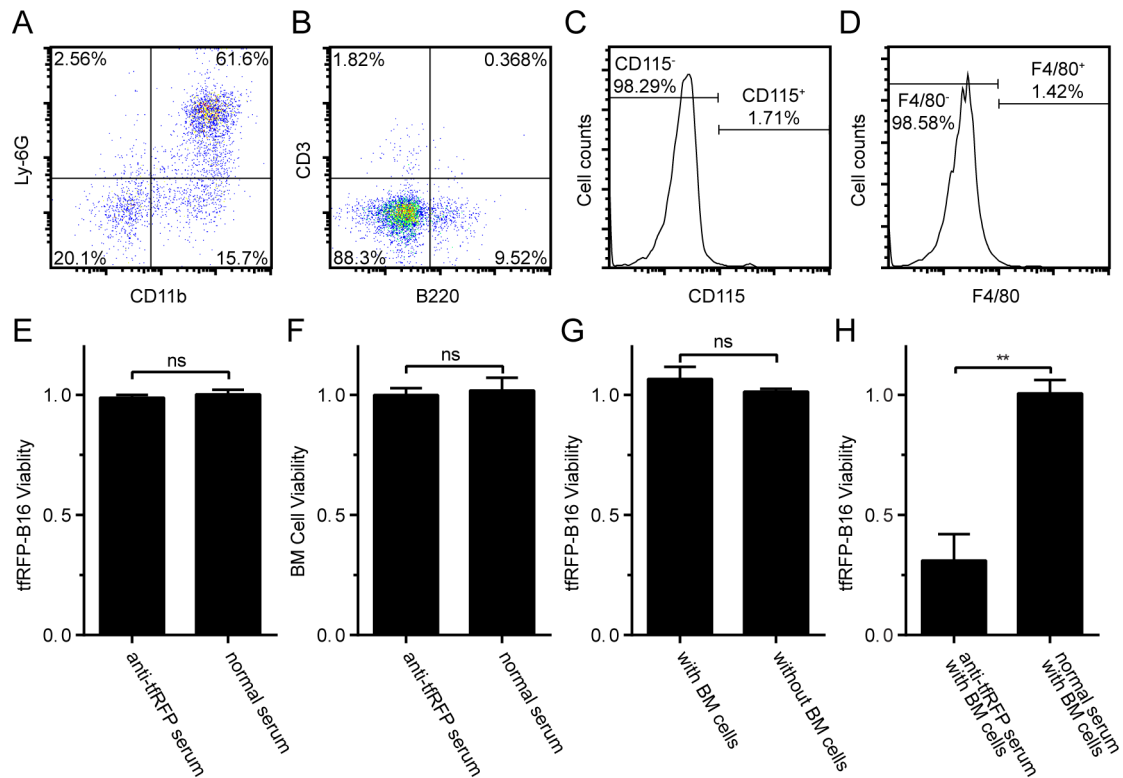


**Figure S11.** ADCC assay using tRF-P-B16 cells with bone marrow cells and anti-tRF-P serum. Bone marrow cells were separated with 60% and 70% Percoll. Anti-tRF-P serum (26 - 30 days after the first immunization) and normal serum were collected from the tRF-P-immunized mice and the normal mice, respectively. (A-D) Flow cytometric characterization of the separated bone marrow myeloid cells. The majority of the cells were neutrophils, with few T cells (CD3<sup>+</sup>) or monocytes/macrophages (CD115<sup>+</sup>, F4/80<sup>+</sup>). Bone marrow cells and murine sera were added to tRF-P-B16 cells for a 24-h incubation at 37°C. A volume of 120  $\mu$ l of medium containing 20  $\mu$ l of MTS was added to the cells after the supernatants were discarded. The cells were then incubated at 37°C for 2 h. The absorption at 490 nm was measured with a Tecan GENios Microplate Reader. (E-H) The cell viability of tumor cells in the indicated experiments. The tRF-P-B16 tumor cells could be killed only in the presence of both bone marrow cells and anti-tRF-P serum. The data shown were pooled from three independent experiments. The values are shown as the means  $\pm$  SEM. Differences with *P* values less than 0.05 were considered statistically significant. (\**P* < 0.05, \*\**P* < 0.01).

**Video S1.** EGFP<sup>+</sup> immunocyte motility in the tumor microenvironment of tRF-P-immunized and non-immunized mice on Day 2. The size of the grid is 50  $\mu$ m  $\times$  50  $\mu$ m. The images were captured at 10 sec/frame with time-lapse two-photon microscopy. The video is played at 100 times real time speed, i.e. 10 frames/sec. Green, EGFP<sup>+</sup> immunocytes; Red, tRF-P-B16 cells.

**Video S2.** EGFP<sup>+</sup> immunocyte motility in the tumor microenvironment of tRF-P-immunized and non-immunized

mice on Day 7. The images were captured at 10 sec/frame with time-lapse two-photon microscopy. The size of the grid is  $50\ \mu\text{m} \times 50\ \mu\text{m}$ . The video is played at 100 times real time speed, i.e. 10 frames/sec. Green, EGFP<sup>+</sup> immunocytes; Red, tRFP-B16 cells.

**Video S3.** EGFP<sup>+</sup> immunocytes formed cell clusters in the tumor microenvironment of tRFP-immunized mice. The images were captured at 10 sec/frame with time-lapse two-photon microscopy. The video is played at 100 times real time speed, i.e. 10 frames/sec. Green, EGFP<sup>+</sup> immunocytes; Red, tRFP-B16 cells. The scale bar represents 100  $\mu\text{m}$ .